Earthquake Simulation Tests of a 1:5 Scale 3-Story Masonry-Infilled Reinforced Concrete Frame

Lee, Han-Seon* Woo, Sung-Woo** Heo, Yun-Sup**

ABSTRACT

The objective of this research is to observe the actual response of a low-rise nonseismic moment-resisting masonry-infilled reinforced concrete frame subjected to varied levels of earthquake ground motions. The reduction scale for the model was determined as 1 : 5 considering the capacity of the shaking table to be used. This model was, then, subjected to the shaking table motions simulating Taft N21E component earthquake ground motion, whose peak ground acceleration(PGA) was modified to 0.12g, 0.2g, 0.3g, and 0.4g. The global behavior and failure mode were observed. The lateral accelerations and displacements at each story and local deformations at the critical portions of the structure were measured. Before and after each earthquake simulation test, free vibration tests and white noise tests were performed to find the changes in the natural period of the model.

When the results of the masonry-infilled frame are compared with those of the bare frame, it can be recognized that masonry infills contribute to the large increase in the stiffness and strength of the global structure whereas it also accompanies the increase of earthquake inertia forces. However, it is judged that masonry infills may be beneficial to the performance of the structure since the rate of increase in strength appears to be greater than that of the induced earthquake inertia forces.

Keywords : shaking table, masonry infills, reinforced concrete frame, earthquake
simulation test, natural period

1. INTRODUCTION

Most building structures which are normally medium- to low-rise reinforced concrete (RC) frames in Korea have not been engineered to resist major or moderate earthquake, and the research on the seismic evaluation of these buildings have not been made sufficiently.

Particularly, masonry infill panels have been used in these structures for architectural or aesthetic reasons, and they have been normally considered as nonstructural elements, and their presence has been often ignored by engineers. However, even though they are considered non-structural elements, it has been recognized that the presence of masonry infills may or may not influence the performance of the structure. In most of the current seismic codes, the influence of nonstructural masonry infills is ignored or considered to a very limited extent by engineers.

The performance of the structure, however, can be greatly improved by the increase of strength arising from the masonry infills. On the contrary, this increase in strength also accompanies the increase of the initial stiffness of the structure and thus may results in a adversely increase of the inertia force. However, the damage of the structure may be reduced by dissipating a considerable portion of the input energy in the infilled masonry, but if the configuration of the infills is irregular, they can induce significant local damages to the structural elements.[4] Accordingly, the research on the investigation of the behavior of structures with or without masonry infills has been made.[5], [6], [7]

However, we have still much unknowns about the behavior or the local and global effect of infills on the structure.

In this study, a 3-story reinforced concrete frame which has been in use as a police office building was selected and the seismic responses of a typical portion of this building structure with the masonry infills were observed.

Considering the capacity of the shaking table to be used in earthquake simulation tests, a 1/5 scale model was constructed. Refer to references (8) and (9) for the detailed techniques to construct the model according to the similitude requirements. Also the process and detailed results of the earthquake simulation test of the bare frame model without masonry infills are presented in reference (12). In this paper, the behaviors of a RC frame with masonry infills are observed and compared with those of the bare frame to make clear the influence of the infilled masonry on the structure.

2. EXPERIMENT

2.1 Test Model and Experimental Setup

The test model used for this study has typical non-seismic details including; (1) a lap-splice at the bottom of the column, (2) large spacings of hoops, (3) no hoops in beam-column joints, and (4) no use of 135° seismic hooks. The test facility used for this study is the shaking table system located in Hyundai Institute of Construction Technology. The instrumentations for measuring the response are shown in Table 1. Two displacement transducers and

accelerometers were installed at each floor to measure the effect of torsion due to accidental unsymmetry of two frames. A loadcell was installed in the mid-height of the column of the first story to measure the shear force of each column. To measure the local response such as the end rotation in the possible plastic hinge regions, 16 displacement transducers were used. And also, to measure the strains at the center of the masonry infilled wall, strain guages were diagonally attached in the plane of masonry wall as shown in Figure 1. The mass to be added to the model according to the similitude law was calculated, and steel plates, each of which has the dimension W×D×L = 9cm ×4cm×35cm (9.9 kg), were used as the artificial mass, as shown in Photo 1. Figure 1 shows two layouts of masonry infills in the model. First, earthquake simulation tests were performed with the Fully Infilled Frame (FIF) in Figure 1(a).

Front Elevation

(a) Fully Infilled Frame(FIF)

Front Elevation
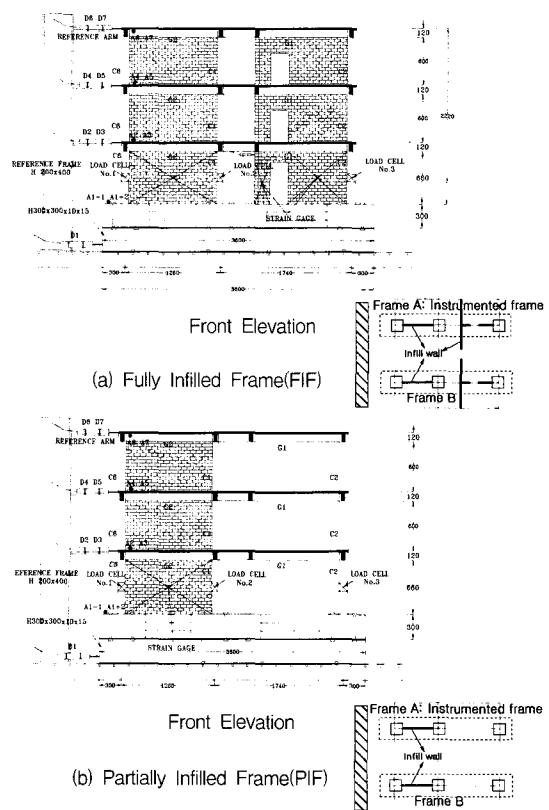
(b) Partially Infilled Frame(PIF)

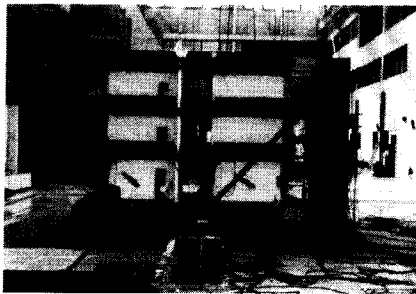Fig.1 Test model and experimental setup(unit: mm)

2.2 Strength Test of Masonry Unit Compressive Strength Test

The type of brick construction was English and the thickness was assumed 1.0B. The prototype brick unit has the dimension of 190mm×90mm×57mm and consists of cement and coarse sand. The strength of 1:5 scale model brick was

made as close to that of prototype as possible by adjusting the mix ratios. The types of tests for the compressive strength of brick(or bricks) and mortar are shown in Figure 2 and the results in Table 3. The average compressive strength of unit model brick turned out to be 14% lower than that of prototype, and the average strength of the model brick

Table 1 Type and number of sensors (unit: ea)

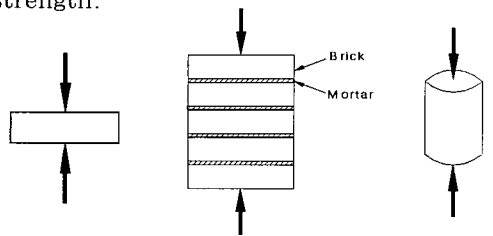|	Displacement transducer (for story drift)	Accelerometer	Load cell	Strain gage	Displacement transducer (for local rotations)
Table	1(D1)	2(A1-1, A1-2)			6 (for beam) 10 (for column) 8 (for masonry infill)
Second Floor	2(D2, D3)	2(A2,A3)			
Third Floor	2(D4, D5)	2(A4,A5)	6	6	
Roof	2(D6, D7)	2(A6,A7)			
Subtotal	7	8	6	6	24
Total: 51					

(a) FIF
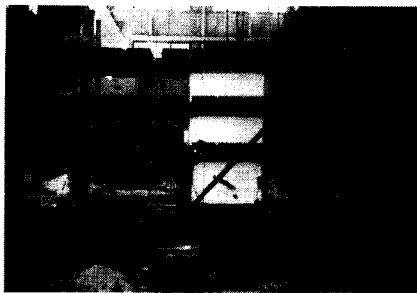
(b) PIF

Photo 1

prism be about 12% higher. From the results of tests for mortar strength, the prototype and the model reveal similar strength.

(a) brick unit   (b) bricks prism   (c) mortar
Fig.2 Types of tests for the compressive strength

Shear Test

According to ASTM (E519-81). specimen for diagonal compression test were manufactured and the instrumentation is shown in Figure 3.Shear tests were performed on both the prototype and the corresponding models of the masonry infills. Test results are shown in Table 4. Comparing the results with the adjustment according to the similitude law, the average strength of the model (1.47×52 = 36.8 tf) was found to be smaller than that of the prototype (49.0 tf). Comparing the Poisson's ratio (ν) estimated at a 1/3 level of the strength, the average Poisson value, ν, of the model (0.38) and that of the prototype (0.29) turned out to be similar. Their failure modes were also found to be similar, as shown in Figure 3(b). Maximum strains in model specimen appear to be larger than those in prototype.

2.3 Experimental Program

The adopted input ground accelerogram is the Taft N2IE component and the peak ground acceleration (PGA) was modified to 0.12g, 0.2g, 0.3g, and 0.4g as shown in Table 5 while the time scale has been compressed according to the similitude

Table 3 Results of compressive strength tests (unit: kgf/cm²)

Type	Brick unit		Brick prism		Mortar	
	Prototype	Model	Prototype	Model	Prototype	Model
average	277.6	238	200	226.9	138.4	140

Table 4 Results of shear tests for the masonry infills

	Prototype				Model			
	Strength (tonf)	Max. Strain (10-6 cm/cm)		ν^*	Strength (tonf)	Max. Strain (10-6 cm/cm)		ν^*
		Horizontal	Vertical			Horizontal	Vertical	
Average	49.0	30	107	0.29	1.47	61	161	0.38

* ν : Poisson's ratio estimated at a 1/3 level of the strength

law. Before and after each earthquake simulation test, free vibration tests were carried out to check the changes of the dynamic characteristic such as the natural period. After finishing the earthquake simulation tests to FIF, the masonry infills with the openings were removed. This partially infilled frame (PIF) as shown in Figure 1(b) was again tested under the same earthquake simulation test program.
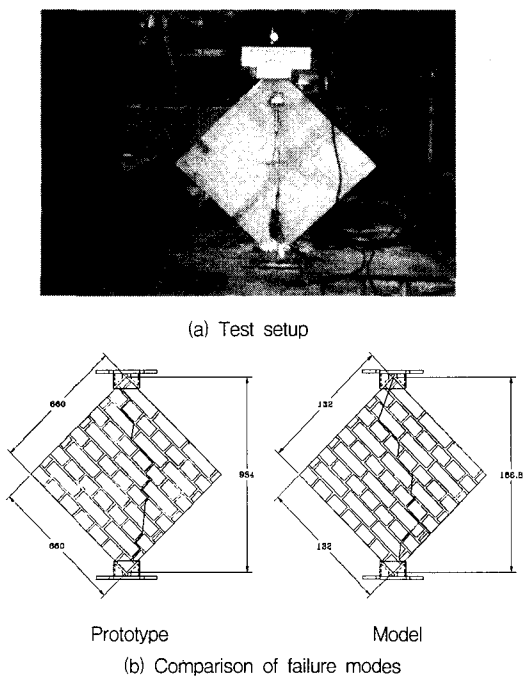

(a) Test setup

Prototype   Model

(b) Comparison of failure modes

Fig.3 Shear test for the masonry infill (unit: mm)

3. EXPERIMENTAL RESULTS AND INTERPRETATION

3.1 Natural Period

The natural periods of FIF and PIF models from the free vibration tests before and after the earthquake simulation test were obtained and compared with the results of the bare frame (BF) model [see Figure 4]. Both FIF and PIF show shorter periods than BF. The period of FIF was found to be the shortest. In FIF, the natural period of the model did not change significantly except the increase after TFT_03 test. In PIF, the natural period was found to increase gradually as the applied peak ground acceleration increase.
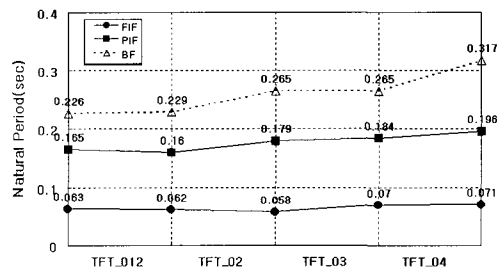
Fig.4 Change of natural periods

3.2 Maximum Floor Drifts and Interstory Drift Ratios

In Figure 5, changes in interstory drifts under the varying peak input accelerations are shown and compared with the values measured in BF. It can be seen from this figure that the drifts of the PIF are greater than those of the FIF under the same level of input ground motions. The comparison of interstory drift ratios (I.D.R's) shows that neither FIF nor PIF exceeds the maximum value

Table 5 Test program

Identification of test	Type(PGA)	Remarks(Return Period)
TFT_012	Taft N21E(0.12g)	Design earthquake in Korea(475 years)
TFT_02	Taft N21E(0.2g)	Max. earthquake in Korea(1000 years)
TFT_03	Taft N21E(0.3g)	Max. considered earthquake in Korea(2000 years)
TFT_04	Taft N21E(0.4g)	Severe earthquake in high-seismicity regions of the world

of 1.5% allowed in the Korean seismic code even under the shake table motions with the PGA 0.4g. Under the shake table motions with PGA 0.12g representing the design earthquake in the current seismic code of Korea, the maximum I.D.R. reveals the value less than 0.3%. Time histories of floor drifts are shown in Figure 6. In this figure, the first mode governs in both FIF and PIF. Also, the drifts in PIF appear to be approximately 3 times those in FIF.
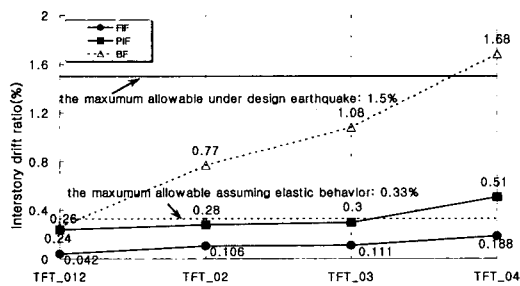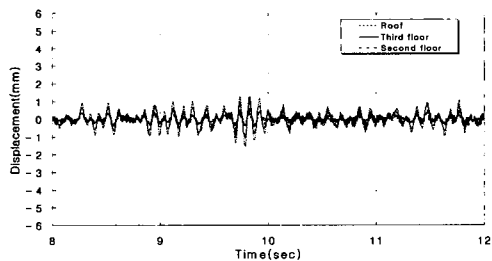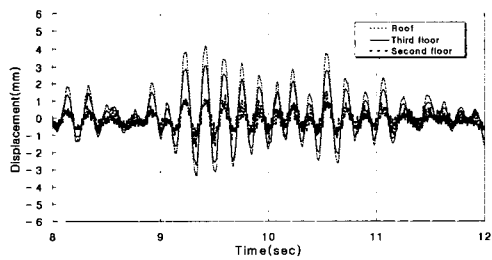

Fig.5 Change of maximum interstory drift ratios

(a) FIF

(b) PIF

Fig.6 Time histories of floor drifts for TFT_02

3.3 Maximum Floor Accelerations and Dynamic Amplification Factor

In Figure 7, the maximum response accelerations at the roof under the shake table motions with the varying peak input accelerations are compared. It can be found that all three models have revealed the trend of decrease in dynamic amplification factors with the increase of the level of shake table motions. The time histories of floor accelerations are shown in Figure 8. It is interesting to note that the third and second floors in PIF show second-mode responses at almost every peak responses of the roof. It is not clear as yet why this phenomenon occurred.
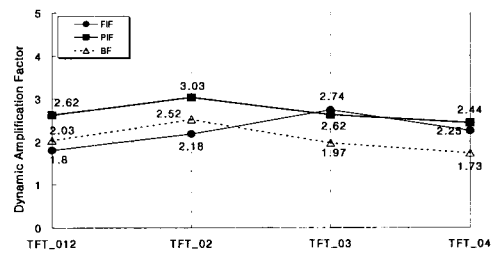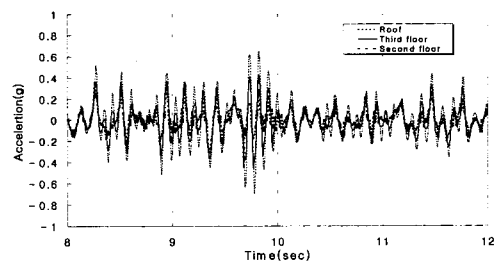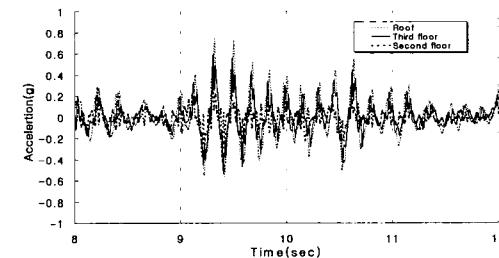

Fig.7 Change of dynamic amplification factor

(a) FIF

(b) PIF

Fig.8 Time histories of floor accelerations for TFT_02

3.4 Base Shear versus Inter-Story Drift at First Story

Figures 9 and 10 show the hysteretic relations between the base shear derived from the measured floor accelerations and the interstory drift at the first story of FIF and PIF. respectively. It can be seen that FIF behaves linear elastically under the table motion simulating PGA 0.12g (TFT_012) which represents the design earthquake in Korea as shown in Figure 9(a). And the maximum base shear was measured to be 3.26 tf, which is about 6.9 times of the design base shear of 0.49 tf. It can also be seen in Figure 10(a), that PIF behaves linear elastically under TFT_012 and the maximum base shear was 3.81 tf, which is about 8.5 times of the design base shear of 0.45 tf. However, it can be noticed that in the case of PIF there are many noises in the drift responses.
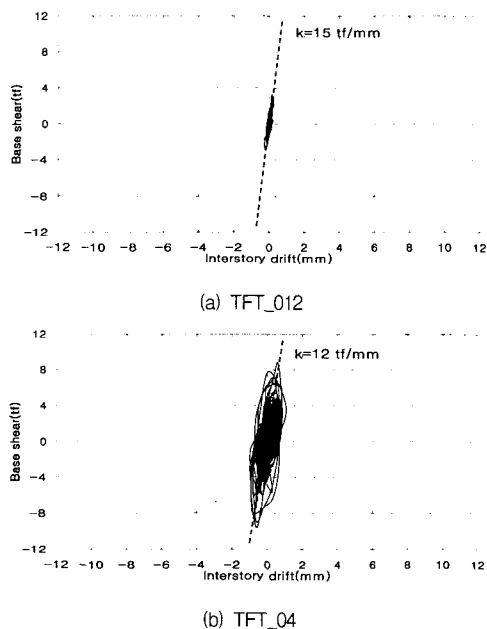

(a) TFT_012

(b) TFT_04

Fig.9 Relation between base shear and interstory drift at first story(FIF)
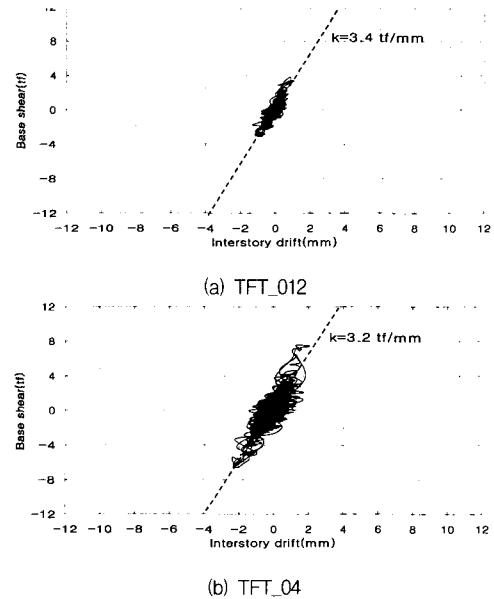

(a) TFT_012

(b) TFT_04

Fig.10 Relation between base shear and interstory drift at first story(PIF)

3.5 Sum of Column Shear versus Base Shear

Figure 11 shows the time histories of the total base shear (the sum of the story inertia forces) and the sum of column shears (the sum of shears measured at load cells) in FIF and PIF under TFT_04, respectively. Similarly Figure 12 compares the hysteretic relation between the interstory drift at the first story and the total base shear obtained by summing the inertia force with that between the interstory drift at the first story and the base shear obtained by summing the shears measured from load cells at the first story columns. It can be seen in Figure 11 that the time history of base shear and column shear are nearly in phase and that the shear carried by the columns are very small compared with the total base shear(7% in FIF and 23% in PIF). This implies that the remaining portions. in other words, the

contributions of the masonry infills to the strength of the global structure are significant. It is also interesting to note in Figure 11 that there is some directional bias in the sum of column shears in the case of PIF while there appears no such bias in FIF. Figure 12 indicates that relatively large energy is dissipated in the hysteretic curve of the total base shear versus I.D.R. at the first story than in that of column shear versus I.D.R. at the same story. The masonry serves as the first line of defence that prevents the damage of the frame by dissipating a considerable portion of energy as well as increases the whole strength of the structure. Besides, the comparison of hysteretic curves of FIF and PIF shows that the whole stiffness of FIF at the first story(12 tf/mm) is about 17 times of the stiffness due to the columns(0.7 tf/mm), whereas that of PIF is about 6 times(3.2 tf/mm : 0.53 tf/mm).
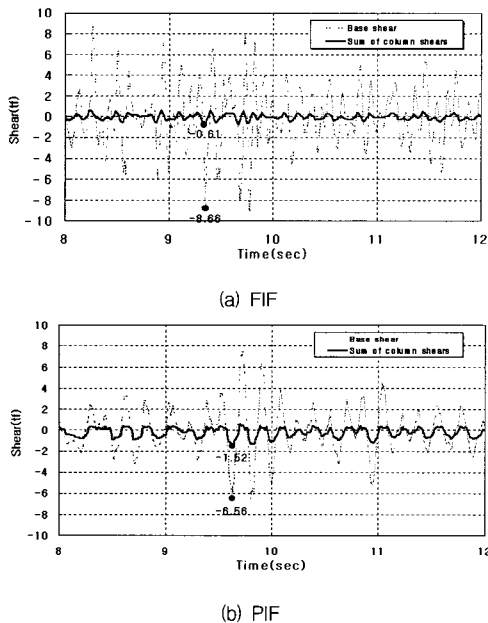

(a) FIF

(b) PIF

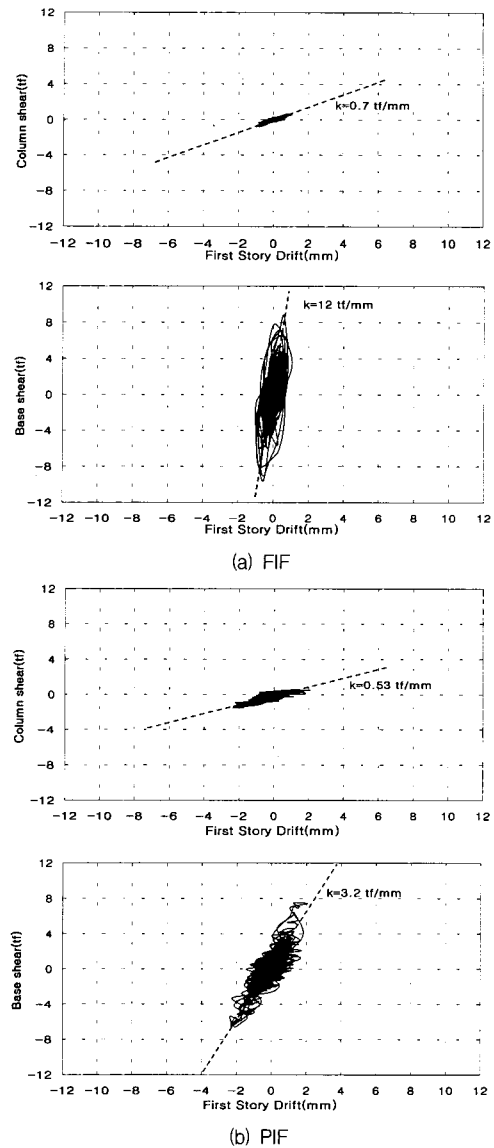Fig.11 Time history of base shear and column shear(TFT_04)

(a) FIF

(b) PIF

Fig.12 Hysteretic relations of base shear versus interstory drift at the first story(TFT_04)

3.6 Ratio of Base Shear to Effective Weight

The ratio of the base shear to the effective weight in this particular case according to the Korean seismic code is as follows.

$$V/W = \frac{AISC}{R} = \frac{(0.12)(1.0)(1.39)}{4.5} = 0.037$$

($T = 0.23 \times \sqrt{5} = 0.514$, $C = \dfrac{1}{1.2\sqrt{T}} = 1.162 \leq 1.5$

$S = 1.2$, $SC = 1.39 \leq 1.75$ $\therefore SC = 1.39$)

Where, V : base shear
W : effective weight of the structure
A : 0.12 (zone factor)
I : 1.0 (importance factor)
T : $0.23 \times \sqrt{5}$ (scale factor)
  = 0.514sec (natural period)
C : $\dfrac{1}{1.2\sqrt{T}} = 1.162 \leq 1.5$ (dynamic factor)
S : 1.2 (soil factor)
SC : 1.39 (but should be less than 1.75.)
R : 4.5 (response modification factor)

Figure 13 shows the trend of the ratio of the base shear to the effective weight for the varying level of the input shake motions. These values are much larger than the design seismic coefficient 0.037 according to the Korean code. The strength of the FIF is approximately over twice of the BF. Even the PIF has the strength 67% larger than that of the BF. Though the damages in the main frame and masonry infills looked minor, the rate of increase in base shear seems to decrease due to the energy dissipation through the frictions between infill walls and frames with the increase of the level of shake table motions.
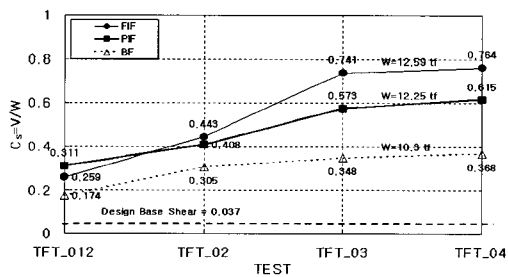

Fig.13 Change of the ratio of max. base shear to effective weight

3.7 Local Responses

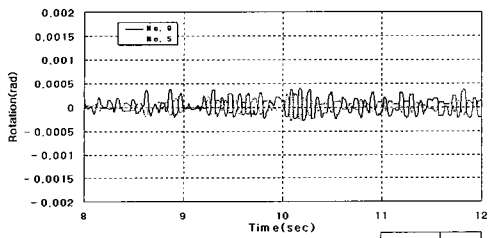Figures 14 shows the example of some time histories of angular rotations in the ends of members and their maximum

values are given in Table 7. The rotational angles were measured over the effective depth d in the ends of beams and the cross-sectional dimension h parallel to the shaking direction in the ends of columns. The maximum rotational angle occurred at the location 4 in case of FIF while that occurred at location 9 in PIF. In any case, the maximum value of rotational angle appeared less than 0.004 rad. From Figure 14, it is noted that the rotations in locations 5 and 9 of PIF are about 4 times larger than those of FIF. It is also observed in case of PIF that the history of rotational angle at location 5 has some bias in the direction whereas that at location 9 does not.

Figures 15 shows the histories of shear forces in the first-story columns. In both FIF and PIF, the shear in the central column whose section is the smallest was found to be the largest. Masonry infill walls reduce the column shear greatly in FIF when compared with the case of PIF. However, the bias in shear can be clearly noticed in PIF due to the effect of the axial compressive forces.
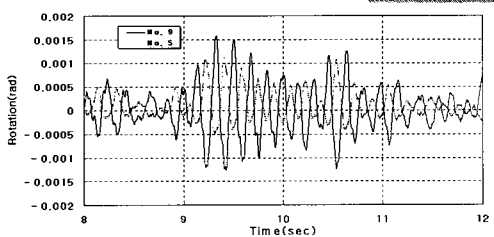
Table 7 Maximum angular rotation (unit: 10^{-5}rad)
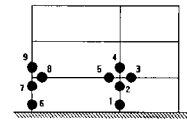
| Test	Location	1 col.	2 col.	3 beam	4 col.	5 beam	6 col.	7 col.	8 beam	9 col.
PGA 0.12g	FIF		29	4	46	15			24	26
	PIF					30	83		36	121
PGA 0.2g	FIF			12	90	28				39
	PIF					112	117	30	74	158
PGA 0.3g	FIF	54	65		64	15		22	21	27
	PIF						156	52	140	226
PGA 0.4g	FIF	74	79		196	32		38	38	33
	PIF					201	185	61	134	316

3.8 Strain of Masonry Infills

Figure 16 shows the measured strains of the masonry infills at the first story for FIF and PIF. In FIF, it can be seen that the strains in the masonry infill wall with openings and cross wall are a little larger than those in the masonry infill wall without openings and cross walls between two columns. It can also be seen that compressive strains appear to be generally twice larger than tensile strains. Compressive strains in PIF appear to be also approximately twice larger than those in FIF.
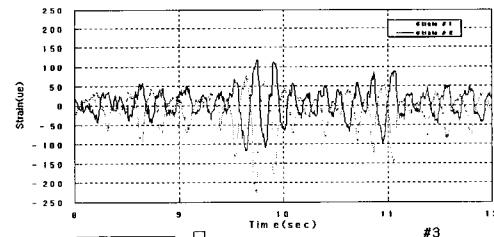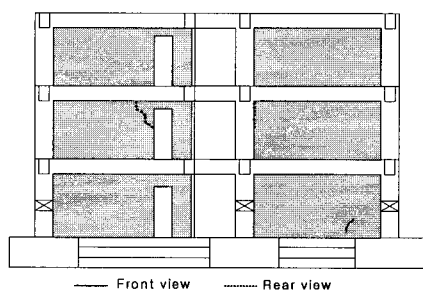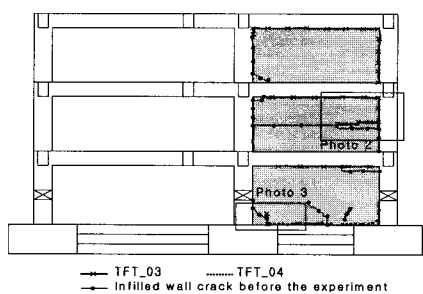

(a) FIF

(b) PIF

Fig.14 Angular rotations under TFT_02
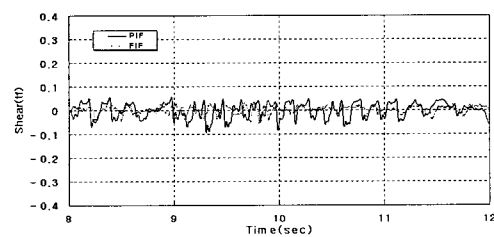
(a) Column No. 1
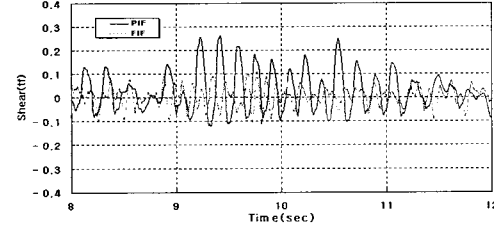
(b) Column No. 2
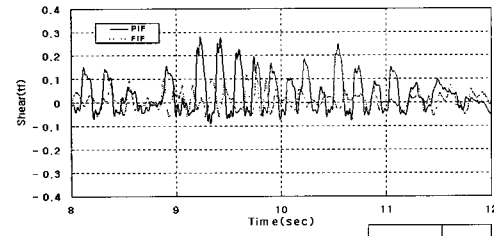
(c) Column No. 3

Fig.15 Column shears under TFT_02
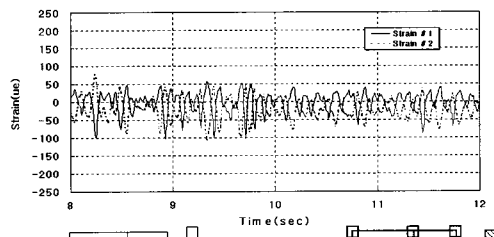
(a) FIF
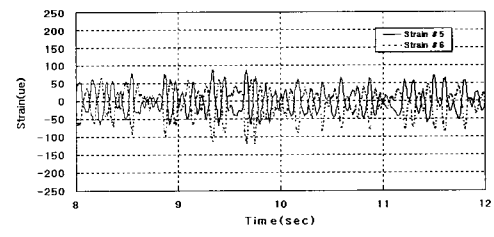
(b) PIF

Fig.16 Strain of the masonry infills at the first story(TFT_04)

3.9 Crack Pattern

The model did not show serious damage even in the case of a severe earthquake (PGA 0.4g) in the high seismic zone of the world. In FIF, several cracks at the masonry infills occurred for TFT_04 as shown in Figure 17(a). In PIF, several cracks at the joints of the masonry infills in each story occurred for TFT_03 and TFT_04 as shown in Figure 17(b).

—— Front view   ········ Rear view

(a) FIF (All after TFT_04)

—— TFT_03   ········ TFT_04
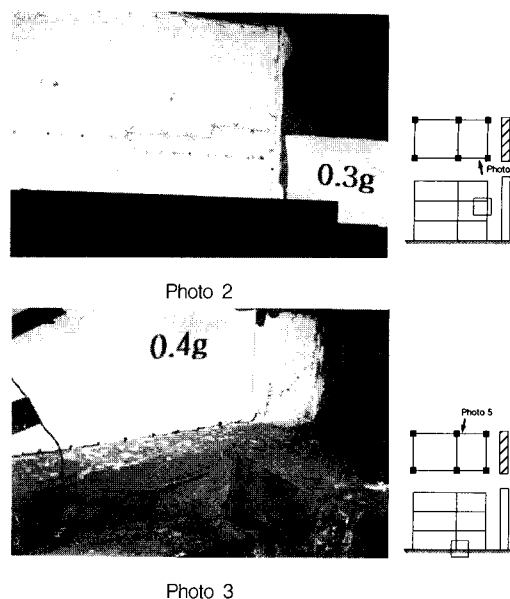—— Infilled wall crack before the experiment

(b) PIF

Fig.17 Crack pattern

4. CONCLUSIONS

The following conclusions have been drawn from the above test results and analyses.

(1) It is found that the masonry infilled building frame structures behave in linear elastically without any damage under the design earthquake prescribed in Korean seismic code.

Photo 2

Photo 3

(2) The natural period and story drift of FIF and PIF were reduced significantly with respect to BF while the maximum floor acceleration, the maximum base shear, and the ratios of V/W greatly increased. It suggests that masonry infills contribute to the large increase in the stiffness and strength of the global structure whereas they accompany also the increase of earthquake inertia forces. However, it is judged that masonry infills may be beneficial to the performance of the structure since the rate of increase in strength appears to be greater than that of the induced earthquake inertia forces.

(3) Even in the case of a severe earthquake (PGA 0.4g), there appeared no significant damage on the masonry infills, nor any damage on the structure.

(4) The influence of infilled masonry walls is so large that it seems to be mandatory to check the effect of infilled masonry wall when building structures should be evaluated realistically with regards to the seismic safety.

ACKNOWLEDGEMENT

REFERENCES

1. Adel G. El-Attar, Richard N. White, and Peter Gergely(1997). "Behavior of Gravity Load Designed Reinforced Concrete Buildings Subjected to Earthquake," ACI Structural J., 94(2), 133-145.
2. Joseph M. Bracci, Andrei M. Reinhorn, and John B. Mander(1995). "Seismic Resistance of Reinforced Concrete Frame Structures Designed for Gravity Loads: Performance of Structural System," ACI Structural J., 92(5), 597-609.
3. V. V. Bertero, A. E. Aktan, A. A.Chowdhury, T. Nagashima(1983). "Experimental and Analytical Characteristics of A 1/5-Scale model of A 7-Story R/C Frame-Wall Building Structure," Rep. No. UCB/EERC-83 /13, Earthquake Engineering Research Center.
4. M.N. Fardis (ed.), "Experimental and numerical investigation on the seismic response of RC infilled frames and recommendations for code provisions", ECOEST/PREC8 Report No. 6, Laboratorio Nacional de Engenharia Civil, Lisbon, 199p, Nov. 1996.
5. Vitelmo Bertero and Steven Brokken, "INFILLS IN SEISMIC RESISTANT BUILDING", Journal of Structural Engineering, Vol. 109, No. 6, June 1983, pp. 1337-1361.
6. M.N. Fardis and T.B. Panagiotakos, "Seismic design and response of bare and infilled reinforced concrete buildings, Part I : Bare structures", J. Earthquake Engng. IC Press 1(1), 219-256 (1997).
7. M.N. Fardis and T.B. Panagiotakos, "Seismic design and response of bare and infilled reinforced concrete buildings, Part II : Infilled structures", J. Earthquake Engng. IC Press 1(3), 475-503 (1997).
8. Kim, S. D., Lee, H. S., Kim, Y. M., and others(1997). "A Study on the Seismic Evaluation and Retrofit of Low-rise Reinforced Concrete Building in Korea," R&D 96-0057, Ministry of Construction and Transportation, Republic of Korea.
9. Lee, H. S., Woo, S. W., and others(1997). "Manufacturing Technique and Material Properties for 1/5-Scale Reinforced Concrete Frame Model," Proceeding of Autumn Conference, 9(2), Korea Concrete Institute, 575-580.
10. Lee, H. S., Woo, S. W., and others(1997). "Shaking Table Tests of A 1/5-Scale 3-Story Nonductile Reinforced Concrete Frame," Proceeding of Autumn Conference, 9(2), Korea Concrete Institute, 581-586.
11. Lee, H. S., Woo, S. W., and Heo, Y. S.(1997). "Inelastic Behaviors of A 3-Story Reinforced Concrete Frame with Nonseismic Details," Proceeding of Spring Conference, 10(1), Korea Concrete Institute, 427-432.
12. Lee, H. S., Woo, S. W., "Earthquake simulation tests of a 1:5 scale gravity load designed 3-story reinforced concrete frame", Journal of the Korea concrete institute, Vol. 10, No. 6, pp241~252, 1998. 12
13. Lee, H. S., Woo, S. W.(1998). "Shaking table tests of a 1/5 scale 3-story nonductile infilled reinforced concrete frame", Proceeding of Autumn Conference, 10(2), Korea Concrete Institute, pp 541~546.